Review article

Heather Goodwin, Tom C. Jellicoe, Nathaniel J.L.K. Davis and Marcus L. Böhm*

Multiple exciton generation in quantum dot-based solar cells

https://doi.org/10.1515/nanoph-2017-0034
Received March 3, 2017; revised June 30, 2017; accepted July 5, 2017

Abstract: Multiple exciton generation (MEG) in quantum-confined semiconductors is the process by which multiple bound charge-carrier pairs are generated after absorption of a single high-energy photon. Such charge-carrier multiplication effects have been highlighted as particularly beneficial for solar cells where they have the potential to increase the photocurrent significantly. Indeed, recent research efforts have proved that more than one charge-carrier pair per incident solar photon can be extracted in photovoltaic devices incorporating quantum-confined semiconductors. While these proof-of-concept applications underline the potential of MEG in solar cells, the impact of the carrier multiplication effect on the device performance remains rather low. This review covers recent advancements in the understanding and application of MEG as a photocurrent-enhancing mechanism in quantum dot-based photovoltaics.

Keywords: multiple exciton generation; quantum dots; solar cells.

1 Introduction

Optimised, large-scale manufacturing processes for the fabrication of photovoltaic devices (PVs) have promoted solar cell technologies to the verge of becoming the cheapest form of energy (4–6 cent/kWh expected by 2025) [1]. While PVs based on materials such as silicon continue to pass economic milestones due to reduced fabrication costs and increased market penetration, the power conversion efficiency (PCE) of these devices is fundamentally limited to around 33% [2, 3]. Means of overcoming this limit, combined with advancements in device manufacturing processes, can progress solar energy technologies towards meeting the growing energy demands of the future.

The fundamental principles of PVs are based upon the concept of a reversible Carnot heat engine. As such, thermodynamics dictates a maximum efficiency limit of 87% for the conversion of solar energy into electrical current [4]. This theoretical performance limit could only be approached in a device architecture where a large number of sub-cells (each optimised for a small section of the solar spectrum) were to be combined in a PV stack and illuminated under intense light concentration [5]. In reality, most PV devices employ only a single cell using one absorbing semiconductor, which collects sunlight under non-concentrated conditions. This non-ideal solar cell environment introduces two dominant loss mechanisms: first, non-absorption of photons with energy less than the semiconductor band gap and secondly, rapid cooling of carriers with energy in excess of the band gap where a portion of the initial photon energy is lost to heat [6]. As a consequence, the ultimate device performance is reduced dramatically from that of an ideal Carnot heat engine.

In their seminal work, Shockley and Queisser quantified the apparent loss processes in a detailed balance model [3]. They expressed the resulting impact on the maximum achievable solar cell efficiency limit in their band gap-dependent Shockley-Queisser model (SQ limit; see Figure 1A).

As light is absorbed in the active layer of a solar cell, excited bound charge-carrier pairs (i.e. excitons) are generated. Before these can be extracted through an external circuit they often encounter loss processes that reduce the efficiency of the solar cell. In the SQ limit, incomplete light trapping or angle restrictions account for up to 20% of all energy losses. It is, however, mainly incomplete absorption and rapid carrier cooling that set the SQ limit for single junction solar cells to maximum PCE of 33.7% for a semiconductor of $E_g \approx 1.3$ eV (see Figure 1A) [6].

*Corresponding author: Marcus L. Böhm, Cavendish Laboratory, University of Cambridge, J. J. Thomson Avenue, Cambridge CB3 0HE, UK, e-mail: mb842@cam.ac.uk
Heather Goodwin and Nathaniel J.L.K. Davis: Cavendish Laboratory, University of Cambridge, Cambridge CB3 0HE, UK
Tom C. Jellicoe: Cavendish Laboratory, University of Cambridge, Cambridge CB3 0HE, UK; and Particle Works, Part of Blacktrace Holdings Ltd., Unit 3, Anglian Business Park, Royston SG8 5TW, UK

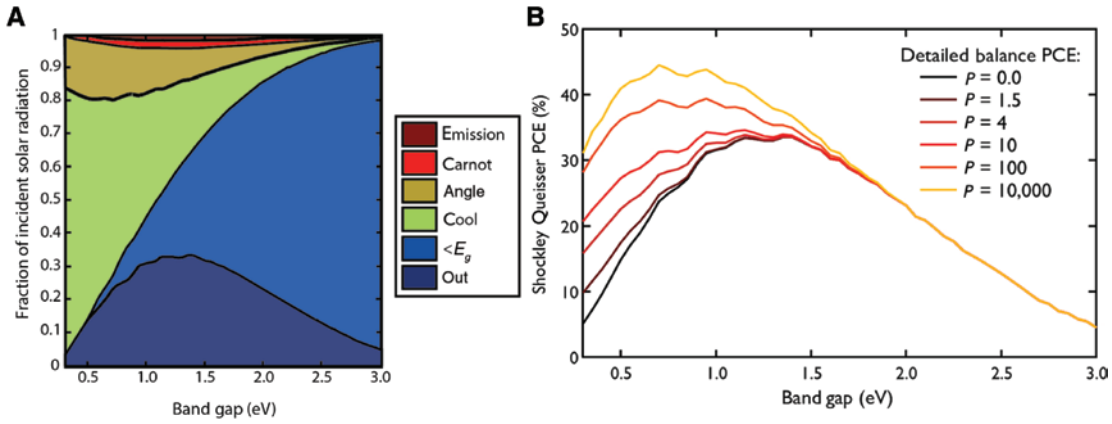

Figure 1: Shockley-Queisser limit: loss processes and potential efficiency enhancement by MEG.
(A) Breakdown of the different loss processes leading to the band gap-dependent Shockley-Queisser limit for single junction solar cells (out, dark blue). $<E_g$ (light blue) and cool (green) represent the energy losses due to incomplete absorption and rapid cooling of hot carriers, respectively, angle (orange) and emission (dark red) are entropic losses associated with angle restriction and incomplete light trapping, respectively, and Carnot (light red) expresses the thermodynamic efficiency limit. (B) Theoretical enhancement of the Shockley-Queisser limit for single junction solar cells due to MEG where the parameter P relates the rates for MEG (k_{MEG}) and hot carrier thermalisation k_{therm} through the expression $P = k_{MEG}/k_{therm}$. Part B has been adapted from [7].

Among the most promising concepts to supress loss processes associated with incomplete absorption are photon up-conversion mechanisms where low energy photons below the band gap are recovered for solar cell operation [8, 9]. As this concept, however, is not within the main focus of this article, we refer the interested reader to other reviews addressing the topic in the literature [10].

The most widely employed approach to reduce losses from rapid cooling is through multi-junction PV devices. These use multiple (usually two or three) semiconductors of different band gaps to best match the solar spectrum [11, 12]. Multi-junction cells have produced PV efficiencies far beyond the SQ limit for single junction solar cells (to date 42% under un-concentrated AM 1.5 G conditions), but their high fabrication cost still renders large-scale deployment challenging [12]. Another concept to minimise losses due to hot carrier cooling is the rapid extraction of the initial hot carriers. While this phenomenon has been theorised to produce superior photovoltages, convincing, experimental evidence for the effect's benefit in a solar cell environment has not been produced yet.

Carrier multiplication (CM) effects, where the energy of a high-energy photon is distributed among multiple carrier pairs with lower energy, present another concept capable of reducing carrier-cooling losses [13–16]. Here, additional charges are produced from energy that would otherwise have been lost as heat. Such processes have been demonstrated to occur efficiently in organic semiconductors and inorganic quantum dots (QDs), where the phenomena are termed singlet exciton fission [17–19] and multiple exciton generation (MEG) [7, 20, 21], respectively. It has been calculated that such CM mechanisms can raise the maximum efficiency of single-junction PVs from about 33% to almost 44% (see Figure 1B) [22].

Several materials and material combinations have been suggested to exploit CM effects in solar cells. Singlet exciton fission materials in combination with suitable charge acceptors and QD-based solar cells have both been shown to produce external quantum efficiencies (EQEs) beyond 100% in a PV device [23–28]. While these proof-of-concept studies show that CM effects can increase the photocurrent of a solar cell, PCEs in both types of device remain low. For MEG in particular, recent spectroscopic findings suggest a combination of high MEG threshold energies and photon energy-dependent MEG efficiency (i.e. MEG efficiency increases slowly after the threshold energy rather than as a step function) as the predominant reasons for the modest contribution to PV power conversion [29, 30].

There are several comprehensive review articles summarising the current understanding of the MEG mechanism itself provided in the literature [29, 31, 32]. In this review, we will only briefly discuss mechanistic details and will focus mainly on recent progress towards an efficient integration of MEG in operational solar cells. After a brief introduction to the process in its nanoscale environment, we will proceed to discussing the underlying device physics of recently reported QD-based solar cells that demonstrate a contribution from MEG to the photocurrent. We will finally provide some material and device-related

suggestions to increase the impact of MEG in future PVs that may enable device performance beyond the SQ limit.

2 Theoretical considerations for promoting MEG in PV devices

2.1 CM in inorganic bulk semiconductors

Upon absorption in bulk semiconductors, solar photons with energy greater than the material band gap E_g generate excited charge-carrier pairs that possess kinetic energy equal to $h\nu - E_g$. They typically dissipate their extra kinetic energy to lattice vibrations on ultra-fast timescales (pico- to sub-pico second regime [33, 34]) as they cool to the band edge. This mechanism is irreversible and is one of the two largest loss processes described in the Shockley-Queisser calculations (see Figure 1A). The idea of replacing this cooling mechanism with an alternative relaxation channel to generate additional charge carriers instead has been theorised since the 1950s [13, 14]. In bulk, this process is understood to be a result of impact ionization (I.I.) where one initial hot carrier (either electron or hole) frees some of its kinetic energy in excess of E_g to excite a second charge carrier across the band gap. For more comprehensive details about I.I. in various bulk materials, we refer the interested reader to the review article by Robbins [35].

Despite the theoretical benefit of I.I. to reduce hot-carrier cooling effects, its impact on device performance is almost negligible in most solar cells. This is mainly due to the I.I. threshold energy E_{th} (i.e. the minimal photon energy required to realise I.I.), which is located in the UV part of the solar spectrum for silicon and most other commercially relevant PV materials ($E_{th}^{silicon} = 3.4\,eV$) [15]. This high E_{th} has been explained by considering the bulk semiconductor's energy and crystal momentum, both of which must be conserved during the generation of additional charge carriers [36]. As only a limited number of solar photons penetrated the earth's atmosphere at these energies, I.I. in current PVs remains insignificant. Furthermore, it has been shown that the efficiency of I.I. is dependent on the energy of the initially absorbed photon in excess of the band gap such that even beyond the threshold energy, the effect is still very small. Since the rate of I.I. competes with carrier cooling on ultra-fast timescales, large excess photon energies are required to render the CM channel competitive [37, 38]. As a consequence, E_{th} has to be considered as a "soft" threshold, which leaves only a fraction of initially created hot carriers subject to I.I. at E_{th} (e.g. in silicon only 5% of hot carriers undergo I.I. at photon energies $h\nu = 4$ eV) [39].

2.2 Enhancing CM in QDs

A different scenario is presented when the semiconductor is confined to the nanoscale where quantum confinement effects can reduce the aforementioned material restrictions for the generation of additional charge-carrier pairs [29, 40]. Quantum confinement effects emerge when the generated excitons are restricted to smaller spatial volumes than they would occupy in the parental bulk material. The natural spatial range over which the excitonic wavefunction spreads is described by the material-dependent Bohr exciton radius. In the quantum confined regime, generation of more than one exciton from a single high energy photon is termed MEG to underline the confined, quasi-excitonic (i.e. non-correlated) character of generated charge carriers [41]. While in bulk materials I.I. is an accepted mechanism, it is not yet clear if the same process is responsible for MEG in quantum-confined materials. The increased efficiency of MEG in these structures has not yet been fully explained and different models have been proposed where the multi-excitonic state is created through an excited virtual multi-excitonic state [42, 43] or via an instantly generated superposition of single- and multi-excitonic state [41, 44].

Interestingly, in QDs, recent spectroscopic findings are indicative of MEG thresholds (E_{th}^{MEG}) being closer to the energy conservation limit ($2E_g$) than in the parental bulk material [30, 31, 45, 46]. In these reports, the authors also find a close correlation between E_{th}^{MEG} and the MEG efficiency (η_{MEG}). While there seems to be general consensus that relaxed crystal momentum conservation rules in quantum-confined materials [47] contribute to E_{th}^{MEG} being close to $2E_g$, there is disagreement in the literature on how other quantum material properties such as discrete energy levels around the QD band gap [47] enhanced coulomb interaction in nanostructures of lower symmetry than spherical QDs [48] or the increased surface-to-volume ratio [49] contribute to the crucial MEG parameters E_{th}^{MEG} and η_{MEG} [50, 51]. What seems clear, however, is that materials with weak charge-phonon coupling (e.g. PbS, PbSe and in particular PbTe) tend to show higher η_{MEG}. This has been explained by a slower hot carrier cooling, which extends the time window for MEG to proceed (see Figure 2). It is worth noting that many of the suggestions to improve E_{th}^{MEG} and η_{MEG} for solar cell applications are based upon ultrafast spectroscopy results that have been collected from solution dispersed QD samples exclusively. As solution-based measurements do not capture all parameters relevant for a material to perform in solar cells, it remains to be seen how efficiencies from the two different environments will correlate. For instance, while

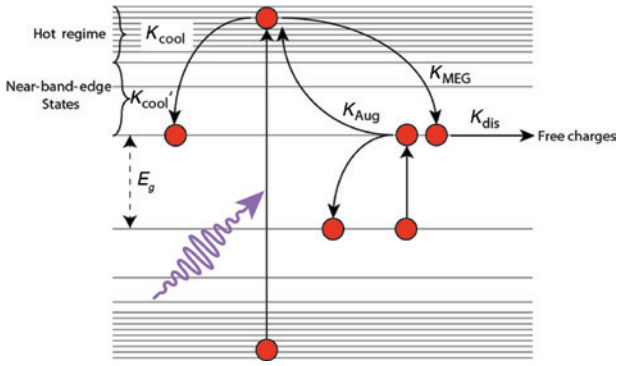

Figure 2: Schematics of the charge-carrier pathways of hot, photogenerated carriers in quantum-confined nanostructures on ultra-fast timescales (<1 ns). After generation, hot charge carriers can either relax to the band edge via rapid carrier cooling (K_{cool}) or can undergo MEG (K_{MEG}). Due to discrete energy levels close to the band gap and a more continuous state distribution higher up in the energy manifold, different hot carrier cooling behaviours can be expected in these two energy regimes which is expressed as K_{cool}' and K_{cool}, respectively. If multiple excitons are generated they either recombine via Auger recombination (K_{Aug}) or dissociate into free charges (K_{dis}), which can then be extracted. Recombination processes operating on longer timescales (e.g. trap-assisted and/or conventional bi-molecular recombination) are not considered here.

increasing the quantum confinement has been shown to boost the efficiency of MEG, it also increases the rate of Auger recombination [52, 53]. On the system level (i.e. in an operational solar cell), strengthening the quantum confinement also weakens the interparticle coupling within the QD film [54] and is thus detrimental for efficient charge extraction. It follows that changing the quantum confinement has an effect not only on the MEG process itself, but also alters device parameters that are crucial for PV performance [29, 49, 54–56].

2.2.1 QD materials for MEG in PV devices

Besides quantum confinement effects, there are other material properties to be considered for MEG on the process and device level. Ideal materials will show relatively slow hot carrier cooling, to extend the time window for MEG (see Figure 2). Additionally, adjusting the Shockley-Queisser calculations to incorporate MEG, Hanna and Nozik showed that the ideal band gap of a photovoltaic material is reduced from around 1.3 to 0.8 eV [22]. To provide good tunability of the quantum confinement in this spectral region, materials with relatively small bulk band gaps are needed.

Whilst MEG has been detected in a number of materials, including silicon [57–59], most studies focused on QDs consisting of lead chalcogenides (PbS, PbSe and PbTe) [26, 41, 60–62]. The large Bohr radius of lead chalcogenides, relative to, for example, silicon or GaAs [59, 63, 64], allows strong quantum confinement effects and efficient tuning of the confinement to produce a band gap in the near-IR region (0.7–1.0 eV) [65]. Furthermore, convenient ligand exchange methods have been established for these particles, giving control over properties of the QD superstructure (e.g. interparticle spacing [55], energy alignment [49], etc.). Together with slow hot carrier cooling, lead chalcogenide QDs are a valuable material platform to study MEG-related parameters not only on the process itself, but also on the PV device level.

2.2.2 Bottlenecks for hot carrier cooling

In most II–VI, III–V and IV–VI semiconductors, it was proposed that the discrete energy levels, produced by quantum confinement, were separated far enough in energy, to require multi-phonon emission events for hot carrier cooling [47]. The low probability of multi-phonon emission was expected to reduce the rate of carrier cooling and therefore extends the time window for MEG and consequently increases its efficiency η_{MEG} [40]. It was shown later that, although in principle this is correct, delayed hot carrier cooling applies mainly to near-band edge states where the quantum confinement produces discrete and far-separated energy levels most efficiently. At energies relevant for MEG (i.e. $>2E_g$) however, the density of states (DOS) is more condensed and should therefore enable rapid carrier cooling via single phonon emission (see Figure 2) [66].

Indeed, the majority of spectroscopic experiments on quantum-confined semiconductors could not necessarily observe delayed hot carrier cooling of photo-generated states far from the band edge. However, recent spectroscopic measurements by Geiregat et al. indicate that quantum-confined lead chalcogenide materials show transiently stable carrier populations at distinct energies high-up in the condensed energy manifold [28, 67]. To explain this transient accumulation of charge carriers far from the band gap, the authors consider a high-energy point in the material's band structure, which requires the relaxing charge carriers to change the direction of the scattering wave vector of the emitted phonons. Interestingly, such an explanation would require at least partial preservation of the bulk phonon dispersion relation in the quantum-confined environment – contradictory to traditional QD theory where momentum conservation is considered as negligible requirement [47].

In PbTe QDs, the energy of this effective phonon scattering bottleneck is approximately at the same position as E_{th}^{MEG}, which has been determined independently under operational solar cell conditions [28]. This transiently stable, hot carrier population close to or above the material's E_{th}^{MEG} extends the time window for MEG. Such a phonon scattering bottleneck is thus consistent with the high MEG yields observed in dispersed PbTe QDs [31, 50, 59] and is also in agreement with the high EQEs (>120%) reported for devices based on the same QD material [28].

2.2.3 Tuning the QD shape to reduce MEG threshold energies

Besides purely, material-based approaches to promote MEG in solar cells, recent reports have shown that the shape control of QDs may provide another path to increase η_{MEG} while reducing E_{th}^{MEG} [26, 30]. Analysing hot carriers in one-dimensional PbSe nanorods has revealed an MEG onset close to the energy conservation limit ($E_{th,rod}^{MEG} = 2.3 - 2.6\,E_g$), which is substantially lower than in comparable, spherical QDs ($E_{th,rod}^{MEG} = 2.7 - 3.2\,E_g$) (see Figure 3A) [46, 68].

To explain such a low E_{th}^{MEG} in nanorods Beard et al. [7] considered an experimentally determined factor P (see Figure 1B) that expresses the competition between the rates of CM k_{MEG} (for $E_{Photon} > E_{th}^{MEG}$) and hot carrier cooling k_{cool}. In this model, increasing k_{MEG} and reducing k_{cool} results in E_{th}^{MEG} approaching the energy conservation limit (i.e. $E_{th}^{MEG} = 2E_g$). While the origin of the lower E_{th}^{MEG} in nanorods is not clear yet, several hypotheses have been discussed in the literature. Stewart et al. consider the rates of MEG (k_{MEG}) and Auger recombination (k_{Aug}), which depend on the DOS of the final states. In case of k_{MEG} that is the DOS of the biexciton (g_2) and in case of k_{Aug} that is the DOS of the hot single exciton (g_1). Due to symmetry reasons the authors suggest that for nanorods there are a larger number of biexciton states accessible in the course of the MEG process, which increases K_{MEG} [69]. Another theory suggests aspect ratio-dependent carrier cooling processes due to reduced carrier-phonon coupling in nanorods [70, 71]. Either hypothesis is in agreement with the observation of a lower E_{th}^{MEG} in nanorods compared to QDs (see Figure 3). However, further experimental work is needed to shed light on the underlying mechanistic details.

Additionally, we note that the empirically determined E_{th}^{MEG} in quantum-confined nanostructures (i.e. spherical QDs and nanorods) by Beard et al. has been determined for lead selenide nanostructures only. It thus remains to be seen if this relation can be generalised to other materials relevant for MEG in PV devices [7].

2.2.4 Impacts of the QD surface on MEG in a device environment

Confining semiconductors on the nanometre scale increases the material's surface-to-volume ratio and this presents challenges for both MEG and QD technologies in general. First, it places a significant proportion of the QD atoms at the surface of the particle. There is general consensus that such an increased number of under-coordinated surface atoms and the relatively small

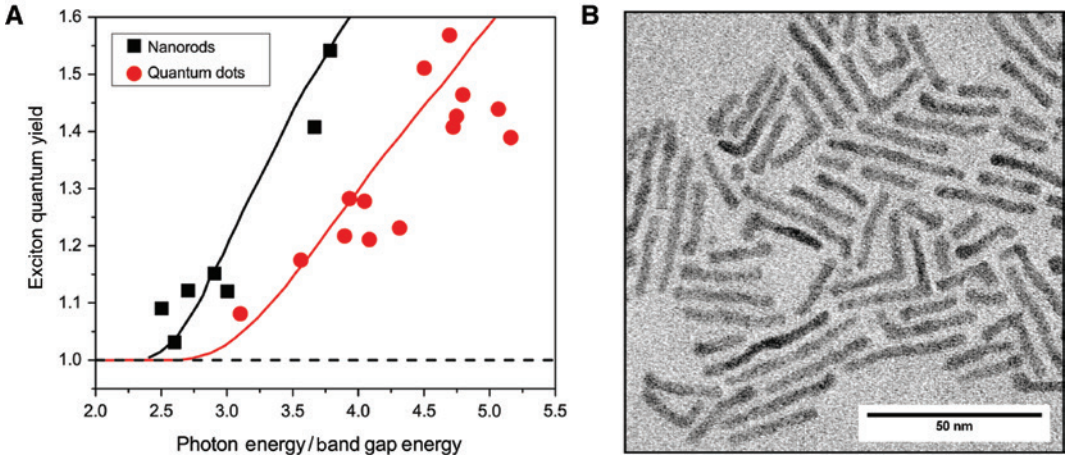

Figure 3: Enhancing quantum yields in 1D nanostructures.
(A) Spectroscopically determined quantum yield of different lead selenide structures as a function of band gap-normalised photon energy. (B) Transmission electron microscopy images of as-synthesised lead selenide nanorods and their different shaped by-products. Part A has been reproduced from data provided in [46] and Part B has been taken from [27].

size of QD surface facets cause the formation of surface states, which are commonly located within the band gap of the semiconductor [47]. Such surface states are generally referred to as tail or trap states and are thought to be responsible for some of the voltage losses associated with QD devices. As the wavefunctions of charge carriers are spatially confined in a smaller volume than in the parental bulk material [49], it follows that the probability of finding charge carriers at the particle surface is greatly increased. The consequence of both effects is that, in QDs, a significant proportion of generated charge carriers will get trapped at surface sites that are energetically removed from the semiconductor's charge transport level [72]. This effect is exacerbated for MEG devices due to the requirement for strong confinement [73, 74].

It is generally accepted that the timescale for relaxing carriers into trap states does not compete with MEG itself (trap filling between 100 s of ps to microseconds depending on QD size and material) [75, 76]. However, surface-trapped carriers can be long-lived species and may therefore nominally charge the QD. Such effects have led to difficulties in measuring MEG rates: a trapped charge may stay on a QD, which upon re-excitation by a subsequent pulse, may form a trion species that can be mistakenly interpreted as an MEG signal thereby complicating spectroscopic studies [43]. In solution-based measurements stirring the sample or the use of a flow cell prevents the same set of QDs being excited by consecutive pulses [61]. In films, however, it remains challenging to isolate effects that influence the MEG process itself, its measurement or the extraction of the generated charges.

Using theoretical calculations, Jaeger et al. showed that $E_{\mathrm{th}}^{\mathrm{MEG}}$ is particularly sensitive to surface defects, most notably non-bonding selenium atoms on the typically lead-rich surface of PbSe QDs [57, 77]. Their calculations showed $E_{\mathrm{th}}^{\mathrm{MEG}}$ to change from $2.6E_g$ to $2.9E_g$ in the presence of surface defects, which is in agreement with experimental results. In addition, Beard et al. demonstrated that η_{MEG} is highly dependent on the QD surface. Altering the surface defect density by using different chemical treatments showed that η_{MEG} can change from 1.0 (i.e. no MEG) to 2.4 [78].

On a more general level, surface trapped carriers are highly localised and are therefore challenging to extract during solar cell operation [79, 80]. Additionally, charge transport properties are intimately linked to the interparticle coupling constant within the QD film [81].

To harvest multiple excitons generated by MEG in a solar cell efficiently, it is thus important to develop strategies for passivating QD surface trap states, while providing sufficient interparticle coupling.

The most widely applied methods to achieve both of these requirements have focused on the materials deployed around the QD core. These strategies use for such surface passivation either a ligand sphere of organic [55, 82, 83] and/or inorganic molecules [49, 80, 84] or a compact, inorganic layer of a wide-band gap semiconductor [62, 85–88].

2.2.4.1 Surface passivation via ligand molecules

In lead chalcogenide QD films, dithiol molecules such as 1,2-ethanedithiol (EDT) or 1,3-benzenedithiol are most commonly used as organic surface ligands to passivate lead-rich cationic surface sites and to provide sufficient interparticle coupling [82, 83, 89]. While QDs passivated with dithiol ligands showed high charge-carrier mobilities [90, 91] and competitive device performances in solar cells, no evidence for MEG could be found in devices [26, 60]. Notably, in QD films where the particles have been treated with EDT exclusively, MEG seemed to be supressed [92]. Interestingly, Tisdale et al. found that PbSe QD films, treated with EDT and placed close to an electron accepting metal oxide (MO) (e.g. TiO_2), show ultrafast, hot electron transfer to the MO [93]. Considering the similar device architecture in common QD-based PV devices where a MO is used as electron acceptor [80, 94, 95], this transfer constitutes another potential hot carrier decay channel competing with MEG and hot carrier cooling (see Figure 2).

It appears that very small surface molecules, such as hydrazine, or even atomic-sized passivants such as halide species, provide efficient surface trap passivation thereby leading to competitive device performance [96–98]. Diamine molecules (instead of dithiols) showed significant MEG yields in films that increased as the length of the diamine ligand was reduced [99]. PVs made using these films, however, do not show clear MEG enhancement to the photocurrent. Instead, supplementing these shorter ligands with longer, thiol-based surface molecules such as mercaptopropionic acid [90] or a mixture of EDT and hydrazine [100, 101] shows a clear contribution of MEG, but reduces carrier mobility and overall device efficiency [26–28].

Besides their direct influence on MEG, QD surface species can also have a significant impact on the charge transport properties of QD films. For instance, coordinating ligands of different electrostatic potential changes the surface dipole moment of QDs which can alter the absolute energy level of the particle by up to 0.9 eV [102]. Furthermore, the reducing character of molecules such as hydrazine has been shown to increase the n-type doping density of IV–VI QD films significantly [96]. Most efficient QD-based PV devices employ a heterojunction analogous

to a p-n junction at an interface between an n-type MO and a depleted, p-type QD layer [82, 103, 104]. It follows that the significant, ligand-associated changes in QD energetics and doping level to promote MEG in a device environment (e.g. by using hydrazine) are challenging to accommodate in the current device architecture tailored for highly efficient QD-based solar cells.

2.2.4.2 The impact of core-shell architectures on MEG

Tuning QD properties to promote MEG in PVs through different organic ligands has been explored extensively [26, 27, 100]. There is general consensus that improved QD trap state passivation played a vital role in this improvement particularly in improving the typically poor V_{oc} of QD devices [97, 104]. The most effective method of surface passivation of QDs has been demonstrated to be a lattice-matched, wide band-gap shell material, grown on the particle core [85, 87, 88, 105]. Surprisingly, recent spectroscopic reports on a variety of IV–VI QD core-shell architectures did not find an increased MEG quantum yield (QY) compared to core-only particles [62]. The authors attributed this to a calculated larger DOS, which intensifies the competition between hot carrier cooling and CM and therefore offsets the benefit of a reduced quantity of surface states.

3 MEG in QD-based solar cells

Having reviewed the most relevant theoretical aspects that may increase the photocurrent of QD-based solar cells via MEG, we will now focus on practical demonstration of these concepts in operational PV devices. To date, there are three reports showing the extraction of more than one charge carrier per incident photon in QD-based PVs. These devices therefore provide proof-of-concept studies underlining that MEG can indeed increase the photocurrent of operational solar cells. Each of these reports targets a different concept to modulate the carrier kinetics within the QD film in order to enhance the impact of MEG in a working device. Furthermore, while all three reports use different materials and/or material structures, they broadly follow the conventional PV device concept of a depleted heterojunction. As the latter architectural considerations of conventional QD-based solar cells are not within the focus of this review, we refer the interested reader to other articles provided in the literature [106–108].

3.1 Tailoring the QD ligand chemistry

In their seminal report, Semonin et al. [26] consider PV devices where PbSe QDs with short, di-thiol ligands molecules are paired with an electron-accepting MO. QD layers closest to the anode were treated with ultra-short diamines (see Figure 4A). For QDs with sufficiently narrow band gaps, peak EQEs beyond 100% were measured (Figure 4B). As mentioned above, applying either di-thiol or di-amine as the sole QD ligand did not produce such high EQE values [26, 96].

Considering the high absorption cross-section of QDs in the MEG-relevant energy spectrum ($h\nu_{photon} > 2E_g$),

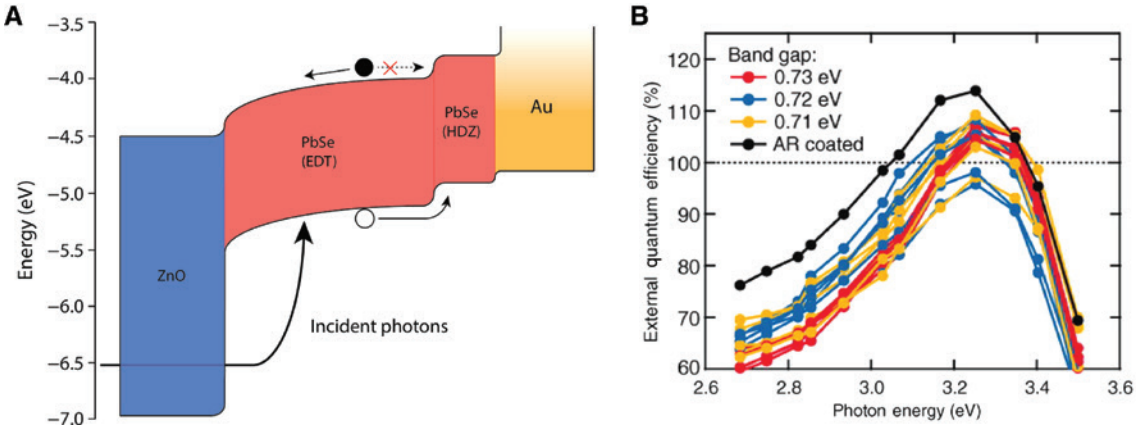

Figure 4: Device architecture and EQEs >100% for PbSe quantum dot-containing solar cells.
(A) Energy landscape of a solar cell based upon PbSe QDs which have been treated with 1,2-ethanedithiol (EDT) or hydrazine (HDZ). The difference in doping density in electron acceptor (ZnO) and QD film produces a depletion region within the QD layer, which drives charge extraction after free carriers have been generated. (B) External quantum efficiency (EQE) of the same PV device architecture showing the high-energy region for three different PbSe QD sizes. All QD sizes demonstrate the generation of more than one carrier produced per incident photon at $h\nu_{photon} = 3.3$ eV. Part B has been taken from [26].

it was argued that photons contributing to MEG are only absorbed in a very thin layer, close to the electron-accepting MO [109]. Such a close proximity to the interface has been shown to favour ultra-fast charge injection (<50 fs) which inhibits MEG loss processes like Auger recombination (see Figure 2) by separating charge carriers before they can recombine [110]. Importantly, tailoring the energetics between MO acceptor and QD donor through surface ligands has been shown to affect this electron transfer rate significantly [111, 112]. Charge transfer rates are commonly influenced not only by the donor-acceptor energetics, but also by the coupling strength between the orbitals involved in the transfer process itself thereby allowing faster charge transfer in stronger coupled partners. Furthermore, applying hydrazine as ligands for particles close to the hole-extracting electrode shifts the QD energetics closer to the vacuum level (see Figure 4A). It follows that the depletion region within the QD film is extended, which increases the efficiency of charge extraction. The second effect of using hydrazine as a ligand is the very short interparticle spacing; this reduces the width of the tunnelling barrier between QDs thereby increasing carrier mobility of the film as a whole. Both effects are particularly beneficial for holes that are produced via MEG as they are commonly located far away from the hole-extracting electrode and are thus prone to recombination during charge extraction [79, 82, 83].

Despite the advantageous effects of a mixed ligand strategy to promote hole extraction, it also reduces the achievable photovoltage of the device. In a conventional QD-based solar cell, the voltage is mainly defined by the quasi-Fermi level splitting between the (mostly p-type) QD donor and the (n-type) MO acceptor at the p-n junction [82, 108]. The increased n-type doping density of the QD film introduced by the hydrazine ligands reduces this splitting and consequently lowers the extractable photovoltage. This is particularly problematic as the V_{oc} in QD-based solar cells is already relatively poor due to other effects such as sub-band gap QD trap states [113] and interfacial trap-states (see Section 4) [79]. Furthermore, while ultra-short ligand molecules increase charge extraction, they also weaken the quantum confinement within the particles, which ultimately interferes with the MEG mechanism itself.

It can thus be concluded at this stage that the reported PbSe QD-based devices provide a first proof-of-concept study for MEG being capable of enhancing the photocurrent in solar cells [26]. However, the depleted heterojunction device architecture [82] presents an issue in that context: whilst strong quantum confinement is required for efficient MEG, this confinement must be weak enough to allow sufficient interparticle coupling for efficient charge (especially hole) extraction.

3.2 Tuning the shape of the QD

One-dimensional, quantum-confined nanostructures (i.e. nanorods) have shown improved MEG efficiencies over spherical QDs not only on the single particle level [45, 46], but also in devices [27]. This has mainly been attributed to two effects: first, the stronger Coulomb matrix element in nanorods, which has been shown to increase MEG without altering the reverse process (i.e. Auger recombination [114]; see Section 2.2.2); secondly, the length of the nanorods themselves aids charge transport as fewer interparticle hopping steps are required to reach the electrodes [115].

Besides the challenge of sufficient surface passivation in these nanostructures, it appears that the preparation of sufficient quantities of high-quality nanorod samples from materials relevant for PV applications is difficult [27]. Among other reasons, the centro-symmetric crystal structure of most commonly used low-band gap QD materials (e.g. the lead chalcogenides PbS, PbSe or PbTe) limits the yield of pure nanorods during synthesis and promotes the formation of side products such as nano-crosses and nano-hooks that are difficult to separate (see Figure 3B) [116].

Despite these synthetic challenges, a recent report demonstrating devices consisting of high-quality PbSe nanorods confirms that MEG in solar cells consisting of non-spherical nanostructures impacts the photocurrent more strongly than in analogous, spherical QD-containing samples [27]. In these devices it is specifically noted that only solar cells where the nanorods have been treated with halides and organic ligands showed clear evidence for MEG in the EQE spectra, again highlighting the importance of careful surface passivation. Additionally, comparing the absorbance-corrected QY or internal quantum efficiency (IQE) of devices containing nanorods showed substantially improved MEG performance over spherical QDs (see Figure 5). Interestingly, PbSe nanorods in the solid state show a sharper increase in QY with photon energy compared to equivalent nanorods in solution despite the fact that device IQEs are typically reduced by Auger recombination competing with charge separation and by regular device recombination losses (see Figure 5). Similar observations have been reported for spherical QDs where the MEG yield of particles in film and solution have been examined via microwave conductivity measurements [117]. Possible explanations for this phenomenon

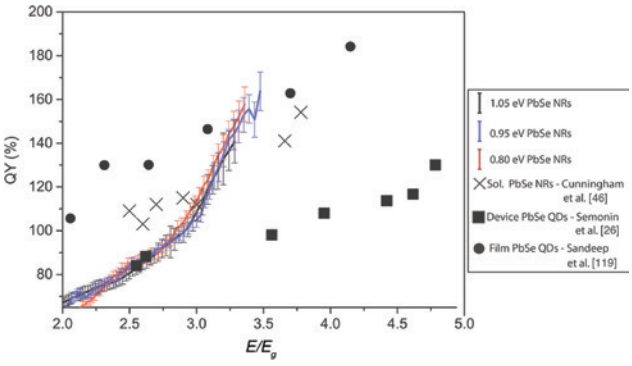

Figure 5: Internal quantum efficiencies (IQEs) of devices based upon PbSe nanorods of three different band gaps (coloured solid lines) and peak quantum yields of devices consisting of spherical PbSe QD (squares). The MEG quantum yields of PbSe nanorods in solution and of spherical PbSe QDs in solid state are shown as crosses and circles, respectively. The figure combines data from [26, 27, 46, 117].

range from the formation of interparticle QD band structures in the solid state [117] to potential trap-assisted MEG mechanisms [118].

An additional difficulty of using nanorods as the main absorber in solar cells involves the deposition of films with adequate optical density and sufficient vertical carrier mobility. It has been shown in films of non-zero dimensional QDs (e.g. nanorods or tetrapods) that local "dead ends" in randomly deposited nanostructures increase the likelihood for carrier recombination thereby limiting carrier extraction [119]. However, large-scale vertical ordering via self-assembly methods has been demonstrated for high-quality nanorod samples [120]. If such a nanostructured film architecture can be fabricated using lead chalcogenide nanorods, it would allow efficient vertical charge extraction whilst taking advantage of the high MEG yields in nanorods.

In addition to QDs and nanorods, there is recent evidence for MEG occurring in two-dimensional nanosheets [121]. While it has been shown that these nanostructures convert the photon energy in excess of $E_{\mathrm{th}}^{\mathrm{MEG}}$ very efficiently into additional charge carriers, these two-dimensional nanosheets require high photon energies to unlock MEG ($E_{\mathrm{th}}^{\mathrm{MEG}} > 3E_g$) – an effect, which renders two-dimensional nanosheets ineffective as sole photon absorbers at this stage.

3.3 The choice of QD material

In a simplified picture, the efficiency of generating multiple-exciton states at early times is mainly influenced by a kinetic competition between the MEG process and ultra-fast hot carrier cooling of the photo-generated state (see Figure 2) [28, 122, 123]. At later times, the multiple-exciton state may then either separate into free carriers or recombine (e.g. via an Auger process). In lead chalcogenide QDs, the latter process proceeds on 20–200 ps time scales [51, 124]. As mentioned previously, charge separation can be at least two orders of magnitude faster if an ionising interface is in close proximity to the generated exciton [110]. Considering the high absorption cross-section of QDs in the spectral region relevant for MEG (i.e. $h\nu_{\mathrm{photon}} > 2E_g$) [109], most multiple-exciton states are conveniently generated close to an interface where a charge accepting material can drive efficient separation. It follows that the separation efficiency of the multiple-exciton states is not systematically limiting further improvements from MEG contributing to the photocurrent.

A different conclusion can be drawn for the early time MEG yield, where different materials have been shown to influence the generation of multi-exciton states via MEG strongly. For instance, spectroscopic results analysing MEG yield in lead chalcogenide QDs after few picoseconds are indicative of a sequentially increasing CM yield within the series PbS, PbSe and PbTe [69]. Although these QY measurements were conducted on particles of similar band gap, the varying Bohr radii of the materials means that this does not equate to the same degree of confinement such that the degree of quantum confinement increases from PbS to PbTe. The observed increase in QY therefore follows the increasing Bohr exciton radii for PbS (18 nm), PbSe (46 nm) and PbTe (150 nm). Furthermore, recent reports confirm that this trend of increased MEG yield is also present in solar cells: incorporating PbTe QDs into working PV devices showed peak EQEs and IQEs ($122 \pm 4\%$ and $155 \pm 7\%$, respectively; see Figure 6A and B) [28], significantly higher than in devices consisting of PbSe QDs of comparable QD band gap (ca. 80% and 95%, respectively) [26].

Based on the stronger quantum confinement present in heavier lead chalcogenide QDs, there is an argument that the stronger matrix element driving the energy transfer process from single- to multiple-excitonic states can explain the higher QYs for PbTe QDs. For the reverse process (i.e. Auger recombination), which is governed by the same matrix element, no difference in recombination timescales as a function of apparent quantum confinement has been found in the series PbS, PbSe and PbTe [31, 69]. Considering ultra-fast exciton separation close to QD-MO interfaces (see Section 3.1) [110] and material independent Auger kinetics, it is conceivable that the higher MEG yields for heavy lead chalcogenide QD devices is due

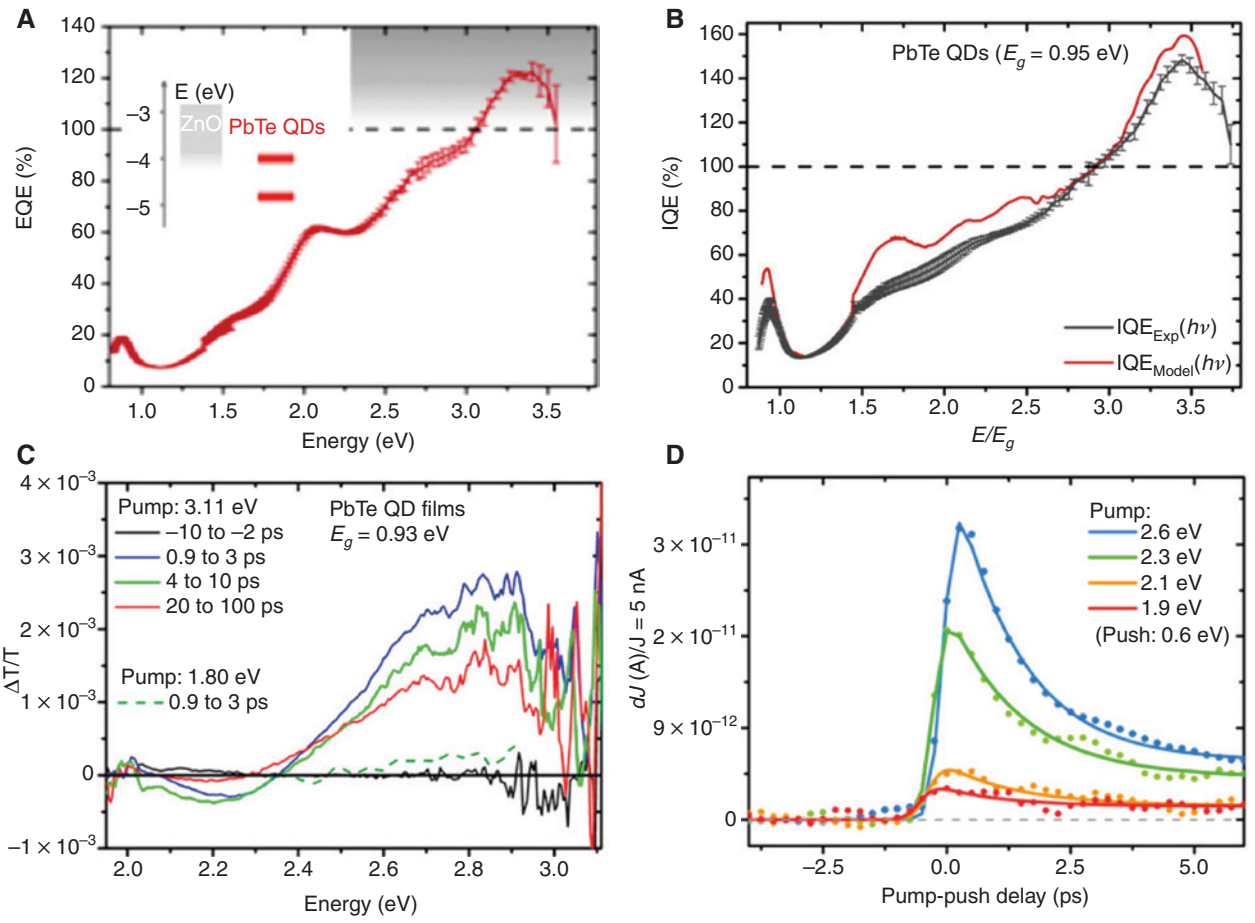

Figure 6: Evidence for carrier multiplication in PbTe quantum dot-containing solar cells.
(A) External and (B) internal quantum efficiencies of PbTe QD-based solar cells. The device architecture is sketched in the inset of (A). IQE_{Exp} ($h\nu$) and IQE_{Model} ($h\nu$) are the internal quantum efficiencies determined via reflectance measurements and via transfer matrix modelling, respectively. (C) Pump-probe transient absorption experiment conducted on films of PbTe QDs suggesting a transiently stable carrier population at about 2.8 eV. (D) Photocurrent response as a function of time delay between excitation pulse and subsequent low-energy push pulse, which re-energises the initial carrier population. All parts of the figure have been taken from [28].

to stronger quantum confinement allowing faster build-up of multiple-excitonic states [31, 69]. These states are then separated efficiently before loss processes such as Auger recombination occur.

Another theory to explain the material-dependent MEG yields in lead chalcogenide QDs is the decreasing frequency of longitudinal optical (LO) phonons in the series PbS, PbSe and PbTe [125]. If the LO phonon frequency becomes too small to bridge the energy gap between the discrete and energetically separated excited states, multi-phonon processes are required to cool the hot carriers, resulting in reduced cooling rates [31, 69]. As mentioned above, these arguments may explain slow carrier cooling at the band edge where the quantum confinement indeed produces discrete and separated states [47]. For the energy regime that is relevant to MEG (i.e. energetically removed from the discretised near-band edge states), these arguments do not hold and therefore cannot explain the apparent difference between the quantum efficiencies of PbSe and PbTe QD-based solar cells [26, 28]. And yet, recent spectroscopic measurement on lead chalcogenide QDs are consistent with a transiently stable carrier population far away from the band edge in the energetically condensed energy manifold (see Figures 2 and 6C) [28, 66]. As briefly discussed above, one explanation for this phenomenon could be the existence of a high-energy point in the material's band structure, which may act as a phonon scattering bottleneck. In this theoretical framework the scattering wave vector of the emitted phonon has to change its direction in order to cool the hot carrier through the "critical" point in the energy manifold. This would increase the number of phonon emission events per energy interval, which consequently reduces the carrier cooling rate [66]. Note that in the context of MEG contributing to the device photocurrent, this bottleneck is only beneficial if it is located at or above E_{th}^{MEG}. Interestingly,

ultra-fast transient photocurrent spectroscopy methods conducted on operational PbTe QDs solar cells and the device IQE characteristics both suggest that at least for PbTe QDs, E_{th}^{MEG} is indeed located at comparable energies to the bottleneck (see Figure 6B–D) [28].

Despite the photophysical advantages associated with PbTe QDs, it remains challenging to integrate these QDs into operational PV devices. One major complication in this context is the material's low oxidation potential, which renders surface oxidation effects highly likely [126]. As a consequence, PV performance limitations such as hindered charge-carrier extraction through the QD film can be expected [127]. The recent demonstration of PV performance recorded from PbTe QD-based solar cells required particle synthesis and device fabrication procedures, where extreme care was taken to exclude oxidising agents of any kind [28].

4 Future directions and outlook

To date all demonstrations of QD-based solar cells showing EQEs beyond unity followed different underlying material paradigms to promote CM in the QD film (i.e. tuning of ligand chemistry, QD shape and material) [26–28]. Besides the QD film designs presented here, there are other promising quantum-confined materials including indium phosphide QDs [7], (6,5) single-walled carbon nanotubes [128] and silicon QDs [58], which show high CM rates at comparably low photon energies (i.e. $E_{th}^{MEG} < E_{th}^{I.I.}$). It is therefore evident that despite the abundance of materials capable of producing high MEG yields, there is no clear picture on what QD properties govern the relevant MEG parameters E_{th}^{MEG} and η_{MEG} in a solar cell [29, 31, 32]. For further improvements in MEG-enhanced PV performance, a deeper understanding of the MEG photophysics is therefore necessary.

An additional problem is the fact that most efforts to integrate the photophysics of MEG into operational solar cells rest upon the same device principle of a depleted heterojunction architecture [26–28]. While this structure has been shown to provide an acceptable compromise between the absorbance- and extraction-limited regime in conventional QD solar cells, different device architectures need to be considered to optimise MEG in PV devices [82, 95, 103, 129]. For instance, the high absorption cross-section of QDs in the energy range relevant for MEG ($>2E_g$) does not require a QD-film thickness of hundreds of nanometres as is common in efficient, conventional QD devices [95, 103, 130]. Furthermore, the major loss processes in conventional QD solar cells (i.e. single-exciton decay and bi-molecular recombination) operate on nano- to microsecond timescales [107]. By contrast, in efficient, MEG-exploiting devices, the separation of the multiple-exciton state and subsequent charge extraction must proceed much faster (<10 s of ps) in order to supress performance-deteriorating processes such as Auger recombination and trion formation. We note that placing a thin (<50 nm) QD film next to a multiple-exciton-ionising interface may accommodate both of these requirements efficiently and consequently enhances the photocurrent contribution of MEG significantly. If, however, the thin QD film is the only photoactive material in the device, the small photon absorption in the single-exciton regime (i.e. $h\nu_{photon} < E_{th}^{MEG}$) is extremely limited allowing only low PV performances [131].

There are several device architectures proposed which could enable MEG to reach PV efficiencies beyond the SQ limit for single junction solar cells. Among the most promising concepts is the photocurrent enhancement of a bottom-contact solar cell [based on a low-band gap absorber (e.g. GaInAs)], using a thin QD film processed on the opposite side of the electrodes (see Figure 7A) [12]. In this architecture most high-energy photons ($h\nu_{photon} > E_{th}^{MEG}$) are absorbed by the QDs thereby allowing the generation of multiple excitons. Placing a bulk semiconductor next to a QD film has been shown to separate and transfer the excitations from the particles into the bulk material [134]. Meanwhile, the remaining low-energy photons, which pass through the QD film can be absorbed by the bulk semiconductor thereby producing charge carriers in a separate process. It follows that in such a tandem-like architecture, CM effects in QDs can supplement the high efficiency of well-known conventional solar cells. We note that a similar tandem-like concept has been proposed for singlet fission-associated CM observed in small organic molecules [135–137]. Despite the observed high quantum yield in some materials (200% in molecular pentacene) [18, 137], it remains challenging to demonstrate energy transfer across the hybrid interface of the tandem-like architecture.

Another concept to exploit MEG more efficiently than in current depleted heterojunction PV devices considers a nanostructured heterointerface between QDs and a charge accepting material (see Figure 7B). Key to this architecture is that the device parameters relevant for photon absorption and multi-exciton separation do not compete along the same direction. Consequently, no trade-off in QD film thickness has to be made between absorption- and extraction-limited regimes. For instance, long nanowires of for example a metal oxide allow deep percolation

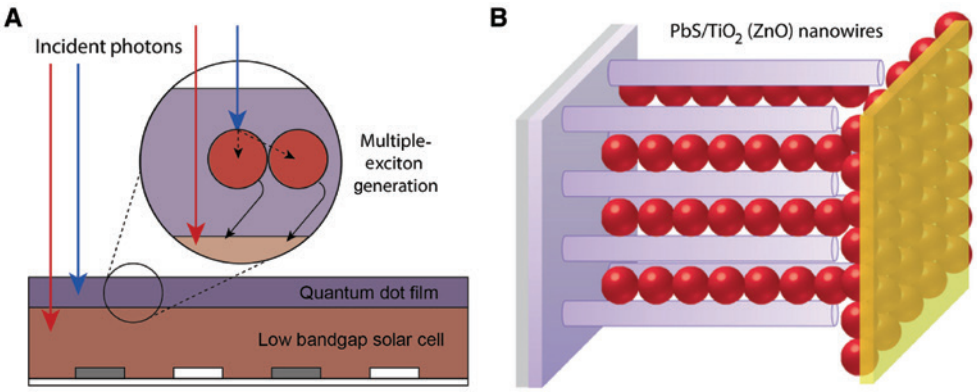

Figure 7: Potential methods for upgrading state-of-the-art solar cells utilising carrier multiplication in quantum dots.
Schematics of (A) an MEG-enhanced, interdigitated bottom-contact solar cell [132]. High-energy photons (blue arrows) are absorbed in the thin QD layer processed on top of a bulk semiconductor where they can undergo MEG. The carriers from the generated multi-exciton state are subsequently transferred to the low band gap semiconductor and can contribute to the photocurrent. Meanwhile, photons of lower energy are more likely to pass through the QD film due to the lower absorption cross-section and can be absorbed and converted into charge carriers in the bulk semiconductor. (B) A device concept based upon a nanostructured hetero-interface between QD absorber and metal oxide acceptor. Here most multiple-exciton states are generated close to an ionising interface. Both an efficient harvest of multi-exciton states and long optical path lengths for absorbing solar photons are possible. Part B is taken from [133].

of QDs thereby creating a long optical path for efficient photon absorption [138]. At the same time, all QDs are placed close to an ionising interface with the MO, which guarantees fast separation of the generated multi-excitons. There are, however, challenges which still need to be overcome (i.e. many shunting pathways due to long and non-uniform nanowires [139] and enhanced trap-mediated recombination caused by the significantly increased interfacial area) [79]. It can be concluded at this stage that adopting QD solar cell architectures according to a tandem-like principle or a nanostructured device environment may enable MEG to contribute to the photocurrent of a PV device more efficiently.

And yet, it is possible that these photocurrent improvements may not be sufficient to promote QD materials to relevant players in the PV market of the imminent future. Instead of boosting the photocurrent via processes like MEG, it appears that minimising losses to the photovoltage maybe a more important factor for advancing solar cell technology in the mid-term. That is due to recently emerging concepts based on rigorous light-trapping techniques [140], solar photon concentration [141] and highly luminescent semiconductors [132, 142], which are already being introduced in present day's PV market [143]. Similarly, techniques to reduce photovoltage losses in QD-based solar cells are put in the research focus of an increasing number of groups [95, 104]. Interestingly, the resulting highly efficient solar cells do not necessarily rely on a fully depleted QD film for charge extraction but function similar to conventional bulk semiconductor devices where carrier diffusion is responsible for efficient charge transport to the electrodes. It is worth noting that these improvements have been the result of refined QD material synthesis and deposition techniques, but increasingly due to adjustment in the device architecture [104, 144].

5 Conclusions

To conclude, MEG has been shown to be a promising, photophysical process to increase the extractable photocurrent in a solar cell. However, even within the reports discussed here, the impact of MEG on the overall device performance remains low; challenges such as a "soft" and high MEG thresholds as well as non-ideal device architectures have restricted the potential of CM in QD devices. Unravelling the detailed mechanism of MEG in an environment, which also considers device relevant parameters (e.g. internal field, ionising interfaces, etc.), will be an important scientific milestone in the near future. Furthermore, conventional QD-based PVs have been developed within an architectural framework allowing efficient charge extraction on nano- and microsecond timescales. To exploit MEG in a device environment more efficiently, measures to accommodate the relevant requirements for efficient CM, multi-exciton separation on sub-picosecond timescales and carrier extraction require further research. It remains to be seen if alternative structures, such as tandem-like architectures or nanostructured device environments, will fully realise MEG in QD-based devices thereby driving PV performances beyond the Schockley-Queisser limit for single junction solar cells.

Acknowledgements: The authors acknowledge Dr. Akshay Rao for useful discussion. HG thanks the EPSRC Centre for Doctoral Training in New and Sustainable Photovoltaics (CDT-PV) for support and funding. This work was supported by the EPSRC and the Winton Program for the Physics of Sustainability. MLB thanks the Sackler and Cambridge Foundation for a Research Fellowship.

References

[1] Mayer JN. Current and future cost of photovoltaics. Long-term scenarios for market development, system prices and LCOE of utility-scale PV systems. Fraunhofer ISE 2015:1–82.
[2] Tanaka A. Technology roadmap – solar photovoltaic energy. International Energy Agency (IEA) 2010:1–42.
[3] Shockley W, Queisser HJ. Detailed balance limit of efficiency of *p-n* junction solar cells. J Appl Phys 1961;32:510–9.
[4] Belghachi A. Solar cells – new approaches and reviews. INTECH, 2015;2:47–76.
[5] Vos A De. Detailed balance limit of the efficiency of tandem solar cells. J Phys D Appl Phys 1980;13:839–46.
[6] Polman A, Atwater HA. Photonic design principles for ultrahigh-efficiency photovoltaics. Nat Mater 2012;11:174–7.
[7] Beard MC, Luther JM, Semonin OE, Nozik AJ. Third generation photovoltaics based on multiple exciton generation in quantum confined semiconductors. Acc Chem Res 2013;46:1252–60.
[8] Mahato P, Monguzzi A, Yanai N, Yamada T, Kimizuka N. Fast and long-range triplet exciton diffusion in metal–organic frameworks for photon upconversion at ultralow excitation power. Nat Mater 2015;14:1–8.
[9] Wu M, Congreve DN, Wilson MWB, et al. Solid-state infrared-to-visible upconversion sensitized by colloidal nanocrystals. Nat Photonics 2016;10:31–4.
[10] Schulze TF, Schmidt TW. Photochemical upconversion: present status and prospects for its application to solar energy conversion. Energy Environ Sci 2015;8:103–25.
[11] Baur C, Bett AW, Dimroth F, et al. Triple-junction III–V based concentrator solar cells: perspectives and challenges. J Sol Energy Eng 2007;129:258–65.
[12] Dimroth F, Grave M, Beutel P, et al. Wafer bonded four-junction GaInP/GaAs//GaInAsP/GaInAs concentrator solar cells with 44.7% efficiency. Prog Photovolt Res Appl 2014;22:277–82.
[13] Antoncik E. On the theory of the spectral dependence of the quantum efficiency of homopolar crystals. Czech J Phys 1957;7:674–89.
[14] Vavilov VS. On photo-ionization by fast electrons in germanium and silicon. J Phys Chem Solids 1959;8:223–6.
[15] Kolodinski S, Werner JH, Wittchen T, Queisser HJ. Quantum efficiencies exceeding unity due to impact ionization in silicon solar cells. Appl Phys Lett 1993;63:2405–7.
[16] Brendel R, Werner JH, Queisser HJ. Thermodynamic efficiency limits for semiconductor solar cells with carrier multiplication. Sol Energy Mater Sol Cells 1996;41–42:419–25.
[17] Merrifield RE, Avakian P, Groff RP. Fission of singlet excitons into pairs of triplet excitons in tetracene crystals. Chem Phys Lett 1969;3:386–8.
[18] Wilson MWB, Rao A, Ehrler B, Friend RH. Singlet exciton fission in polycrystalline pentacene: from photophysics toward devices. Acc Chem Res 2013;46:1330–8.
[19] Smith MB, Michl J. Singlet fission. Chem Rev 2010;110:6891–936.
[20] Schaller RD, Klimov VI. High efficiency carrier multiplication in PbSe nanocrystals: implications for solar energy conversion. Phys Rev Lett 2004;92:186601.
[21] Nozik AJ. Quantum dot solar cells. Phys E 2002;14:115–20.
[22] Hanna MC, Nozik AJ. Solar conversion efficiency of photovoltaic and photoelectrolysis cells with carrier multiplication absorbers. J Appl Phys 2006;100:74510.
[23] Congreve DN, Lee J, Thompson NJ, et al. External quantum efficiency above 100% in a singlet-exciton-fission-based organic photovoltaic cell. Science 2013;340:334–7.
[24] Tabachnyk M, Ehrler B, Bayliss S, Friend RH, Greenham NC. Triplet diffusion in singlet exciton fission sensitized pentacene solar cells. Appl Phys Lett 2013;103:153302–4.
[25] Yang L, Tabachnyk M, Bayliss SSL, et al. Solution-processable singlet fission photovoltaic devices. Nano Lett 2014;15:354–8.
[26] Semonin OE, Luther JM, Choi S, et al. Peak external photocurrent quantum efficiency exceeding 100% via MEG in a quantum dot solar cell. Science 2011;334:1530–3.
[27] Davis NJLK, Böhm ML, Tabachnyk M, et al. Multiple-exciton generation in lead selenide nanorod solar cells with external quantum efficiencies exceeding 120%. Nat Commun 2015;6:8259.
[28] Böhm ML, Jellicoe TC, Tabachnyk M, et al. Lead telluride quantum dot solar cells displaying external quantum efficiencies exceeding 120%. Nano Lett 2015;15:7987–93.
[29] Smith C, Binks D. Multiple exciton generation in colloidal nanocrystals. Nanomaterials 2013;4:19–45.
[30] Beard MC, Midgett AG, Hanna MC, Luther JM, Hughes BK, Nozik AJ. Comparing multiple exciton generation in quantum dots to impact ionization in bulk semiconductors: implications for enhancement of solar energy conversion. Nano Lett 2010;10:3019–27.
[31] Padilha LA, Stewart JT, Sandberg RL, et al. Carrier multiplication in semiconductor nanocrystals: influence of size, shape, and composition. Acc Chem Res 2013;46:1261–9.
[32] Schaller RD, Agranovich VM, Klimov VI. High-efficiency carrier multiplication through direct photogeneration of multi-excitons via virtual single-exciton states. Nat Phys 2005;1:189–94.
[33] Doany FE, Grischkowsky D. Measurement of ultrafast hot-carrier relaxation in silicon by thin-film-enhanced, time-resolved reflectivity. Appl Phys Lett 1988;52:36–8.
[34] Price MB, Butkus J, Jellicoe TC, et al. Hot-carrier cooling and photoinduced refractive index changes in organic–inorganic lead halide perovskites. Nat Commun 2015;6:8420.
[35] Robbins DJ. Aspects of the theory of impact ionization in semiconductors (I). Phys Stat Sol 1980;79:9–50.
[36] Wolf M, Brendel R, Werner JH, Queisser HJ. Solar cell efficiency and carrier multiplication in Si_{1-x} Ge_x alloys. J Appl Phys 1998;83:4213.
[37] Bude J, Hess K. Thresholds of impact ionization in semiconductors. J Appl Phys 1992;72:3554–61.
[38] Würfel P. Solar energy conversion with hot electrons from impact ionisation. Sol Energy Mater Sol Cells 1997;46:43–52.
[39] Christensen O. Quantum efficiency of the internal photoelectric effect in silicon and germanium. J Appl Phys 1976;47:689–95.

[40] Nozik AJ. Spectroscopy and hot electron relaxation dynamics in semiconductor quantum wells and quantum dots. Annu Rev Phys Chem 2001;52:193–231.
[41] Ellingson RJ, Beard MC, Johnson JC, et al. Highly efficient multiple exciton generation in colloidal PbSe and PbS quantum dots. Nano Lett 2005;5:865–71.
[42] Rupasov VI, Klimov VI. Carrier multiplication in semiconductor nanocrystals via intraband optical transitions involving virtual biexciton states. Phys Rev B – Condens Matter Mater Phys 2007;76:125321–6.
[43] McGuire JA, Joo J, Pietryga JM, Schaller RD, Klimov VI. New aspects of carrier multiplication in semiconductor nanocrystals. Acc Chem Res 2008;41:1810–9.
[44] Shabaev A, Efros A, Nozik A. Multiexciton generation by a single photon in nanocrystals. Nano Lett 2006;6:2856–63.
[45] Padilha LA, Stewart JJT, Sandberg RRL, et al. Aspect ratio dependence of auger recombination and carrier multiplication in PbSe nanorods. Nano Lett 2013;13:1092.
[46] Cunningham PD, Boercker JE, Foos EE, et al. Enhanced multiple exciton generation in quasi-one-dimensional semiconductors. Nano Lett 2011;11:3476–81.
[47] Alivisatos AP. Semiconductor clusters, nanocrystals, and quantum dots. Science 1996;271:933–7.
[48] Bartnik AC, Efros AL, Koh WK, Murray CB, Wise FW. Electronic states and optical properties of PbSe nanorods and nanowires. Phys Rev B – Condens Matter Mater Phys 2010;82:1–16.
[49] Böhm ML, Jellicoe TC, Rivett J, et al. Size and energy level tuning of quantum dot solids via a hybrid ligand complex. J Phys Chem Lett 2015;6:3510–4.
[50] Murphy JE, Beard MC, Norman AG, et al. PbTe colloidal nanocrystals: synthesis, characterization, and multiple exciton generation. J Am Chem Soc 2006;128:3241–7.
[51] Stewart JT, Padilha LA, Qazilbash MM, et al. Comparison of carrier multiplication yields in PbS and PbSe nanocrystals: the role of competing energy-loss processes. Nano Lett 2012;12:622–8.
[52] Klimov VI. Quantization of multiparticle auger rates in semiconductor quantum dots. Science 2000;287:1011–3.
[53] Robel I, Gresback R, Kortshagen U, Schaller RD, Klimov VI. Universal size-dependent trend in auger recombination in direct-gap and indirect-gap semiconductor nanocrystals. Phys Rev Lett 2009;102:1–4.
[54] Beard MC. Multiple exciton generation in semiconductor quantum dots. J Phys Chem Lett 2011;2:1282–8.
[55] Böhm ML, Kist RJP, Morgenstern FSF, et al. The influence of nanocrystal aggregates on photovoltaic performance in nanocrystal-polymer bulk heterojunction solar cells. Adv Energy Mater 2014;4:1400139.
[56] Damtie FA, Karki KJ, Pullerits T, Wacker A. Optimization schemes for efficient multiple exciton generation and extraction in colloidal quantum dots. J Chem Phys 2016;145:064703–5.
[57] Jaeger HM, Fischer S, Prezhdo OV. Decoherence-induced surface hopping. J Chem Phys 2012;136:22A545–14.
[58] Trinh MT, Limpens R, de Boer WDAM, Schins JM, Siebbeles LDA, Gregorkiewicz T. Direct generation of multiple excitons in adjacent silicon nanocrystals revealed by induced absorption. Nat Photonics 2012;6:316–21.
[59] Beard MC, Knutsen KP, Yu P, et al. Multiple exciton generation in colloidal silicon nanocrystals. Nano Lett 2007;7:2506–12.
[60] Law M, Luther JM, Beard MC, Choi S, Nozik AJ. Solar cells based on colloidal quantum dot solids: seeking enhanced photocurrent. Conf Rec IEEE Photovolt Spec Conf 2009:002068–73.
[61] Midgett AG, Hillhouse HW, Hughes BK, Nozik AJ, Beard MC. Flowing versus static conditions for measuring multiple exciton generation in PbSe quantum dots. J Phys Chem C 2010;114:17486–500.
[62] Trinh MT, Polak L, Schins JM, et al. Anomalous independence of multiple exciton generation on different group IV – VI quantum dot architectures. Nano Lett 2011;11:1623–9.
[63] Liu Z, Sun Y, Yuan J, et al. High-efficiency hybrid solar cells based on polymer/PbSxSe1-x nanocrystals benefiting from vertical phase segregation. Adv Mater 2013;25:5772–8.
[64] Honold A, Schultheis L, Kuhl J, Tu CW. Collision broadening of two-dimensional excitons in a GaAs single quantum well. Phys Rev B 1989;40:6442–5.
[65] Jasieniak J, Califano M, Watkins SE. Size-dependent valence and conduction band-edge energies of semiconductor nanocrystals. ACS Nano 2011;5:5888–902.
[66] Pandey A, Guyot-Sionnest P. Slow electron cooling in colloidal quantum dots. Science 2008;322:929–32.
[67] Geiregat P, Delerue C, Justo Y, et al. A phonon scattering bottleneck for carrier cooling in lead chalcogenide nanocrystals. ACS Nano 2015;9:778–88.
[68] Sandberg RL, Padilha LA, Qazilbash MM, et al. Multiexciton dynamics in infrared-emitting colloidal nanostructures probed by a superconducting nanowire single-photon detector. ACS Nano 2012;6:9532–40.
[69] Stewart JT, Padilha LA, Bae WK, Koh WK, Pietryga JM, Klimov VI. Carrier multiplication in quantum dots within the framework of two competing energy relaxation mechanisms. J Phys Chem Lett 2013;4:2061–8.
[70] Kelley AM. Electron – phonon coupling in CdSe nanocrystals. J Phys Chem Lett 2010;1:1296–300.
[71] Lange H, Mohr M, Artemyev M, Woggon U, Niermann T, Thomsen C. Optical phonons in colloidal CdSe nanorods. Phys Status Solidi Basic Res 2010;247:2488–97.
[72] Oh SJ, Berry NE, Choi JH, et al. Stoichiometric control of lead chalcogenide nanocrystal solids to enhance their electronic and optoelectronic device performance. ACS Nano 2013;7:2413–21.
[73] Midgett AG, Luther JM, Stewart JT, et al. Size and composition dependent multiple exciton generation efficiency in PbS, PbSe, and PbSxSe1–xAlloyed quantum dots. Nano Lett 2013;13:3078–85.
[74] Nozik AJ. Multiple exciton generation in semiconductor quantum dots. Chem Phys Lett 2008;457:3–11.
[75] Bakulin AA, Neutzner S, Bakker HJ, Ottaviani L, Barakel D, Chen Z. Charge trapping dynamics in PbS colloidal quantum dot photovoltaic devices. ACS Nano 2013;7:8771–9.
[76] Burda C, Link S, Mohamed M, El-Sayed M. The relaxation pathways of CdSe nanoparticles monitored with femtosecond time-resolution from the visible to the IR: assignment of the transient features by carrier quenching. J Phys Chem B 2001;105:12286–92.
[77] Jaeger HM, Hyeon-deuk KIM, Prezhdo OV. Exciton multiplication from first principles. Accounts 2013;46:1280–9.
[78] Beard MC, Midgett AG, Law M, Semonin OE, Ellingson RJ, Nozik AJ. Variations in the quantum efficiency of multiple exciton

generation for a series of chemically treated PbSe nanocrystal films. Nano Lett 2009;9:836–45.
[79] Ehrler B, Musselman KP, Böhm ML, et al. Preventing interfacial recombination in colloidal quantum dot solar cells by doping the metal oxide. ACS Nano 2013;7:4210–20.
[80] Ip AH, Thon SM, Hoogland S, et al. Hybrid passivated colloidal quantum dot solids. Nat Nanotechnol 2012;7:577–82.
[81] Li H, Zhitomirsky D, Shreya D, et al. Toward the ultimate limit of connectivity in quantum dots with high mobility and clean gaps. ACS Nano 2016;10:606–14.
[82] Pattantyus-Abraham A, Kramer I. Depleted-heterojunction colloidal quantum dot solar cells. ACS Nano 2010;4:3374–80.
[83] Koleilat GI, Levina L, Shukla H, et al. Efficient, stable infrared photovoltaics based on solution-cast colloidal quantum dots. ACS Nano 2008;2:833–40.
[84] Liu Y, Gibbs M, Perkins CL, et al. Robust, functional nanocrystal solids by infilling with atomic layer deposition. Nano Lett 2011;11:5349–55.
[85] Chen O, Zhao J, Chauhan VP, et al. Compact high-quality CdSe–CdS core–shell nanocrystals with narrow emission linewidths and suppressed blinking. Nat Mater 2013;12:445–51.
[86] Yanover D, Čapek RK, Rubin-Brusilovski A, et al. Small-sized PbSe/PbS core/shell colloidal quantum dots. Chem Mater 2012;24:4417–23.
[87] Reiss P, Protière M, Li L. Core/shell semiconductor nanocrystals. Small 2009;5:154–68.
[88] Neo DCJ, Cheng C, Stranks SD, et al. Influence of shell thickness and surface passivation on PbS/CdS core/shell colloidal quantum dot solar cells. Chem Mater 2014;26:4004–13.
[89] Moreels I, Fritzinger B, Martins JC, Hens Z. Surface chemistry of colloidal PbSe nanocrystals. J Am Chem Soc 2008;130:15081–6.
[90] Jeong KS, Tang J, Liu H, et al. Enhanced mobility-lifetime products in PbS colloidal quantum dot photovoltaics. ACS Nano 2012;6:89–99.
[91] Klem EJD, Shukla H, Hinds S, MacNeil DD, Levina L, Sargent EH. Impact of dithiol treatment and air annealing on the conductivity, mobility, and hole density in PbS colloidal quantum dot solids. Appl Phys Lett 2008;92:1–4.
[92] Law M, Beard MC, Choi S, Luther JM, Hanna MC, Nozik AJ. Determining the internal quantum efficiency of PbSe nanocrystal solar cells with the aid of an optical model. Nano Lett 2008;8:3904–10.
[93] Tisdale WA, Williams KJ, Timp BA, Norris DJ, Aydil ES, Zhu X-Y. Hot-electron transfer from semiconductor nanocrystals. Science 2010;328:1543–7.
[94] Kirmani AR, Carey GH, Abdelsamie M, et al. Effect of solvent environment on colloidal-quantum-dot solar-cell manufacturability and performance. Adv Mater 2014;26:4717–23.
[95] Maraghechi P, Labelle AJ, Kirmani AR, et al. The donor–supply electrode enhances performance in colloidal quantum dot solar cells. ACS Nano 2013;7:6111–6.
[96] Talapin DV, Murray CB. PbSe nanocrystal solids for n- and p-channel thin film field-effect transistors. Science 2005;310:86–9.
[97] Bae WK, Joo J, Padilha LA, et al. Highly effective surface passivation of PbSe quantum dots through reaction with molecular chlorine. J Am Chem Soc 2012;134:20160–8.
[98] Woo JY, Ko J-H, Song JH, et al. Ultrastable PbSe nanocrystal quantum dots viain situformation of atomically thin halide adlayers on PbSe(100). J Am Chem Soc 2014;8:8883–6.
[99] Ten Cate S, Sandeep CSS, Liu Y, et al. Generating free charges by carrier multiplication in quantum dots for highly efficient photovoltaics. Acc Chem Res 2015;48:174–81.
[100] Ono M, Nishihara T, Ihara T, et al. Impact of surface ligands on the photocurrent enhancement due to multiple exciton generation in close-packed nanocrystal thin films. Chem Sci 2014;5:2696.
[101] Gao Y, Aerts M, Sandeep CSS, et al. Photoconductivity of PbSe quantum-dot solids: dependence on ligand anchor group and length. ACS Nano 2012;6:9606–14.
[102] Brown PR, Kim D, Lunt RR, et al. Energy level modification in lead sulfide quantum dot thin films through ligand exchange. ACS Nano 2014;8:5863–72.
[103] Chuang C, Brown P, Bulović V, Bawendi M. Improved performance and stability in quantum dot solar cells through band alignment engineering. Nat Mater 2014;13:796–801.
[104] Liu M, Voznyy O, Sabatini R, et al. Hybrid organic–inorganic inks flatten the energy landscape in colloidal quantum dot solids. Nat Mater 2017;16:258–63.
[105] Ning Z, Gong X, Comin R, et al. Quantum-dot-in-perovskite solids. Nature 2015;523:324–8.
[106] Tang J, Sargent EH. Infrared colloidal quantum dots for photovoltaics: fundamentals and recent progress. Adv Mater 2011;23:12–29.
[107] Kramer IJ, Sargent EH. The architecture of colloidal quantum dot solar cells: materials to devices. Chem Rev 2014;114:863–82.
[108] Carey GH, Abdelhady AL, Ning Z, Thon SM, Bakr OM, Sargent EH. Colloidal quantum dot solar cells. Chem Rev 2015;115:12732–63.
[109] Leatherdale CA, Woo WK, Mikulec FV, Bawendi MG. On the absorption cross section of CdSe nanocrystal quantum dots. J Phys Chem B 2002;106:7619–22.
[110] Yang Y, Rodríguez-Córdoba W, Xiang X, Lian T. Strong electronic coupling and ultrafast electron transfer between PbS quantum dots and TiO_2 nanocrystalline films. Nano Lett 2012;12:303–9.
[111] Anderson NA, Lian T. Ultrafast electron transfer at the molecule-semiconductor nanoparticle interface. Annu Rev Phys Chem 2005;56:491–519.
[112] Morgenstern FSF, Böhm ML, Kist RJP, et al. Charge generation and electron-trapping dynamics in hybrid nanocrystal-polymer solar cells. J Phys Chem C 2016;120:19064–9.
[113] Chuang CHM, Maurano A, Brandt RE, et al. Open-circuit voltage deficit, radiative sub-bandgap states, and prospects in quantum dot solar cells. Nano Lett 2015;15:3286–94.
[114] Aerts M, Spoor FCM, Grozema FC, Houtepen AJ, Schins JM, Siebbeles LDA. Cooling and auger recombination of charges in PbSe nanorods: crossover from cubic to bimolecular decay. Nano Lett 2013;13:4380–6.
[115] Huynh WU, Dittmer JJ, Alivisatos AP. Hybrid nanorod-polymer solar cells. Science 2002;295:2425–7.
[116] Boercker JE, Foos EE, Placencia D, Tischler JG. Control of PbSe nanorod aspect ratio by limiting phosphine hydrolysis. J Am Chem Soc 2013;135:15071–6.
[117] Sandeep CSS, ten Cate S, Schins JM, et al. High charge-carrier mobility enables exploitation of carrier multiplication in quantum-dot films. Nat Commun 2013;4:2360.
[118] Allan G, Delerue C. Fast relaxation of hot carriers by impact ionization in semiconductor nanocrystals: role of defects. Phys Rev B 2009;79:195324.

[119] Hindson JC, Saghi Z, Hernandez-Garrido J-C, Midgley PA, Greenham NC. Morphological study of nanoparticle – polymer solar cells using high-angle annular dark-field electron tomography. Nano Lett 2011;11:904–9.
[120] Baker JL, Widmer-Cooper A, Toney MF, Geissler PL, Alivisatos AP. Device-scale perpendicular alignment of colloidal nanorods. Nano Lett 2010;10:195–201.
[121] Aerts M, Bielewicz T, Klinke C, et al. Highly efficient carrier multiplication in PbS nanosheets. Nat Commun 2014;5:3789.
[122] Schaller RD, Petruska MA, Klimov VI. Effect of electronic structure on carrier multiplication efficiency: comparative study of PbSe and CdSe nanocrystals. Appl Phys Lett 2005;87:1–3.
[123] Allan G, Delerue C. Role of impact ionization in multiple exciton generation in PbSe nanocrystals. Phys Rev B – Condens Matter Mater Phys 2006;73:1–5.
[124] Nootz G, Padilha LA, Levina L, et al. Size dependence of carrier dynamics and carrier multiplication in PbS quantum dots. Phys Rev B – Condens Matter Mater Phys 2011;83:1–7.
[125] Dalven R. Energy-gap anomaly in the semiconductor sequence PbS, PbSe, and PbTe. Phys Rev B 1971;3:3359–67.
[126] Bode D, Levinstein H. Effect of oxygen on the electrical properties of lead telluride films. Phys Rev 1954;96:259–65.
[127] Konstantatos G, Howard I, Fischer A, et al. Ultrasensitive solution-cast quantum dot photodetectors. Nature 2006;442:180–3.
[128] Kanemitsu Y. Multiple exciton generation and recombination in carbon nanotubes and nanocrystals. Acc Chem Res 2013;46:1358–66.
[129] Ning Z, Dong H, Zhang Q, Voznyy O, Sargent EH. Solar cells based on inks of n-type colloidal quantum dots. ACS Nano 2014;8:10321.
[130] Ning Z, Voznyy O, Pan J, et al. Air-stable n-type colloidal quantum dot solids. Nat Mater 2014;13:822–8.
[131] Sambur JB, Novet T, Parkinson BA. Multiple exciton collection in a sensitized photovoltaic system. Science 2010;330:63–6.
[132] Pazos-Outon LM, Szumilo M, Lamboll R, et al. Photon recycling in lead iodide perovskite solar cells. Science 2016;351:1430–3.
[133] Lan X, Masala S, Sargent EH. Charge-extraction strategies for colloidal quantum dot photovoltaics. Nat Mater 2014;13;233–40.
[134] Sun B, Findikoglu AT, Sykora M, Werder DJ, Klimov VI. Hybrid photovoltaics based on semiconductor nanocrystals and amorphous silicon. Nano Lett 2009;9:1235–41.
[135] Tabachnyk M, Ehrler B, Gélinas S, et al. Resonant energy transfer of triplet excitons from pentacene to PbSe nanocrystals. Nat Mater 2014;13:1033.
[136] Thompson NJ, Wilson MWB, Congreve DN, et al. Energy harvesting of non-emissive triplet excitons in tetracene by emissive PbS nanocrystals. Nat Mater 2014;13:1039–43.
[137] Tabachnyk M, Karani AH, Broch K, et al. Efficient singlet exciton fission in pentacene prepared from a soluble precursor. APL Mater 2016;4:116112.
[138] Wang H, Kubo T, Nakazaki J, Kinoshita T, Segawa H. PbS-quantum-dot-based heterojunction solar cells utilizing ZnO nanowires for high external quantum efficiency in the near-infrared region. J Phys Chem Lett 2013;4:2455–60.
[139] Jean J, Chang S, Brown PR, et al. ZnO nanowire arrays for enhanced photocurrent in PbS quantum dot solar cells. Adv Mater 2013;25:2790–6.
[140] Tamang A, Hongsingthong A, Sichanugrist P, et al. On the potential of light trapping in multiscale textured thin film solar cells. Sol Energy Mater Sol Cells 2016;144:300–8.
[141] Liu L, Barber GD, Shuba MV, et al. Planar light concentration in micro-si solar cells enabled by a metallic grating–photonic crystal architecture. ACS Photonics 2016;3:604–10.
[142] Miller OD, Yablonovitch E, Kurtz SR. Strong internal and external luminescence as solar cells approach the shockley–queisser limit. IEEE J Photovolt 2012;2:303–11.
[143] Gielen D. Concentrating solar power. International Renewable Energy Agency (IRENA) working paper 2012;1:1–48.
[144] Lan X, Voznyy O, Kiani A, et al. passivation using molecular halides increases quantum dot solar cell performance. Adv Mater 2016;28:299–304.